# Solvent-Induced Surface Morphology of Thin Polymer Films

**P. Müller-Buschbaum,**[*,†] **J. S. Gutmann,**[‡,§] **M. Wolkenhauer,**[‡] **J. Kraus,**[‡] **M. Stamm,**[§]
**D. Smilgies,**[||] **and W. Petry**[†]

*Physik-Department, LS E13, TU München, James-Franck-Strasse 1, 85747 Garching, Germany;
Max-Planck-Institut für Polymerforschung, Ackermannweg 10, 55128 Mainz, Germany; Institut für
Polymerforschung e.V., Hohe Strasse 6, 01069 Dresden, Germany; and ESRF, BP 220,
38043 Grenoble, France*

*Received May 25, 2000; Revised Manuscript Received October 31, 2000*

ABSTRACT: With specular and off-specular X-ray scattering the surface morphology in terms of surface roughness, film quality, and roughness correlation in thin polymer films of polystyrene and fully brominated polystyrene is measured. During the preparation of the thin films on top of silicon substrates, the common solvent was varied. We investigated eight different solvents and three different solvent mixtures to depict the influence of typical solvent parameters. In the regime of a small solvent vapor pressure, we observed correlated roughness as the ultimate lower limit of accessible surface smoothness. The resulting films are homogeneous, and the surface roughness is given by the substrate. In an intermediate vapor pressure regime marked surface morphologies are detected, while at a high vapor pressure smoother films result again.

## Introduction

Thin polymer films are widely used in applications like microelectronics or coatings. Depending on the desired properties of the polymer film, several different experimental techniques for its preparation are developed. One frequently applied technique is the spin coating of a polymer solution. In fundamental investigations, the preparation of thin films by spin coating is a common technique as well. It is used to obtain flat and homogeneous films with film thicknesses down to the radius of gyration of the unperturbed molecule. Despite its importance in fundamental investigation and application the understanding of the spin-coating process had only moderate success. Because of the complex nature of it, major simplifying assumptions had been used in the model description. For example the rheological properties of the solutions used were oversimplified or solvent evaporation was neglected. Although more realistic models include some of these aspects together with a variety of other effects, the agreement with experimental results is still limited.[1−3] In the experimental work, the development of empirical relations, inspired by the aim of obtaining a controlled preparation technique, was focused.[4−6] Unfortunately, these studies were carried out with very specific polymer−solvent systems, where information concerning the polymer and the nature of the interaction between the polymer and the solvent is limited. Basically only the resulting film thickness of the polymer film was under investigation. For example, the rotational speed, the solution viscosity, and the solution concentration were determined to be important parameters, which significantly affect the thickness. The amount of solution initially dispensed onto the substrate, its dispension rate, and the total spinning time as well as the ac-

celeration rate were reported to be negligible. In contrast to the obtained film thickness, the resulting surface roughness was less investigated. In contrast to polymer blend systems the surface morphology for homopolymer films was only rarely examined. Recently, the installation of long-range correlation between the polymer surface and the substrate surface was reported.[7−9] With the ongoing effort in characterization techniques the detection of this special type of surface morphology becomes possible.[10−13] Using off-specular X-ray scattering the dependence of this roughness replication on the molecular weight, film thickness or annealing temperature was determined.[7]

In the present investigation, we focus on the solvent used for spin coating. The morphology is determined in terms of surface roughness, film quality, and roughness correlation. The spin coating was performed with different characteristic solvents.[14] We restrict ourselves to frequently used model polymers like polystyrene and brominated polystyrene. As reported previously,[8] both polymers exhibit roughness correlation if toluene is used as a solvent. In the investigation of eight different solvents as well as three solvent mixtures, typical solvent parameters like viscosity, surface tension, vapor pressure, and electric dipole moment were varied over a broad range.[15] In one set of experiments, the amount of polymer used for the spin coating remained constant. In the other set of experiments, the film thickness of the resulting polymer film was kept constant. The sample surface was investigated with optical microscopy. Additionally the film thickness and the surface morphology were probed with X-ray scattering techniques, which ensures a high resolution as compared to other techniques. The vapor pressure turned out to basically determine the observed morphologies.

This article is structured as follows: The introduction is followed by an Experimental Section describing the sample preparation and the techniques used. The next section gives an introduction into roughness replication. The sections on results and discussion are followed by a summary and an outlook.

* Corresponding author.
† TU München.
‡ Max-Planck-Institut für Polymerforschung.
§ Institut für Polymerforschung e.V.
|| ESRF. Present address: Cornell University, Ithaca, NY.

**Table 1. Characteristic Data of Solvents Used in This Investigation[a]**

| solvent | abbr | $v_p$ (kPa) | $\mu$ (Debye) | $\eta$ (mPa s) | $\gamma$ (mN/m) |
|---|---|---|---|---|---|
| acetone | $C_3H_6O$ | 30.8 | 2.88 | 0.306 | 23.46 |
| tetrahydrofuran | $C_4H_8O$ | 21.6 | 1.75 | 0.456 | 23.97 |
| cyclohexane | $C_6H_{12}$ | 13.0 | 0.0 | 0.912 | 24.65 |
| 1,2-dichloroethane | $C_2H_4Cl_2$ | 10.6 | 1.8 | 0.464 | 31.86 |
| chloroform | $CHCl_3$ | 26.2 | 1.04 | 0.537 | 26.67 |
| toluene | $C_7H_8$ | 3.79 | 0.37 | 0.560 | 27.93 |
| trichloroethylene | $C_2HCl_3$ | 9.91 | 0.8 | 0.545 | 25.18 |
| carbon tetrachloride | $CCl_4$ | 15.2 | 0.0 | 0.908 | 26.43 |

[a] The vapor pressure is denoted with $v_p$, the electric dipole moment with $\mu$, the viscosity with $\eta$, and the surface tension with $\gamma$.

**Table 2. Solvent Mixtures Used in the Presented Investigation**

| solvent 1 | solvent 2 | vol ratio |
|---|---|---|
| acetone | cyclohexane | 50:50 |
| cyclohexane | toluene | 86.9:13.1 |
| methanol | toluene | 80:20 |

## Experimental Section

**Sample Preparation.** The polystyrene (PS) used in this investigation was prepared by anionic polymerization (Max-Planck-Institut für Polymerforschung). From the characterization by gel permeation chromatography (GPS) using calibrated standards results a molecular weight $M_w$ = 28 000 with a narrow molecular weight distribution of $M_w/M_n$(PS) = 1.05. The statistical polystyrene-*stat*-*p*-bromostyrene copolymer (PBrS) with a mole fraction of *p*-bromostyrene of $x$ = 1.09 was prepared by direct electroPsilic bromination of the polystyrene precursors.[16,17] The bromine content was determined by microgravimetric analysis. The calculation from the molecular weight of the PS precursor on the basis of the degree of bromination yields $M_w$ = 144 700 and $M_w/M_n$(PBrS) = 1.04. The thin polymer films were prepared by spin coating of a homogeneous polymer solution. In sample series A, the PS concentration of the solution was kept fixed, which results in different film thicknesses depending on the solvent used. In sample series B, the PBrS concentration was varied to fulfill the boundary condition of a fixed film thickness.[6] The used solvents are listed in Table 1 together with some characteristic parameters. In addition to single solvents, we used binary mixtures of solvents as shown in Table 2.

Prior to spin-coating (1950 rpm for 30 s) the substrates, native oxide covered Si(100) surfaces (MEMC Electronic Materials Inc., Spartanburg, NC), were cleaned in an acid bath. The cleaning bath consists of 100 mL of 80% $H_2 SO_4$, 35 mL of $H_2O_2$ and 15 mL of deionized water. After 15 min at 80° C in the acid bath, the substrates were taken out, rinsed in deionized water, and dried with compressed nitrogen. In the case of using cyclohexane as a solvent, the substrate was heated to 50 °C right before it was placed on the spin coater. Immediately before coating, the dry substrates were flushed with fresh solution. Several samples were prepared out of the same solution. To check the reproducibility of observed structures, several samples were prepared and examined. The very accurate surface cleaning ensures during every repetition of the preparation the detection of statistically the same morphologies. Thus, while each individual sample position shows a different arrangement of the individual surface features, the statistical features of the film morphology remain the same.

**Optical Microscopy.** A detection of large in-plane length scales as compared to SFM was performed with optical microscopy using a Zeiss Axiotech 25H optical microscope with magnifications between 4 and 50 times. A Hitachi KP-D50 CCD camera recorded the micrographs.

**Optical Phase Measurement Interference Microscope.** An optical characterization of the samples was achieved with a LOT/ZYGO phase measurement interference microscope. The interference pattern of monochromatic light reflected from
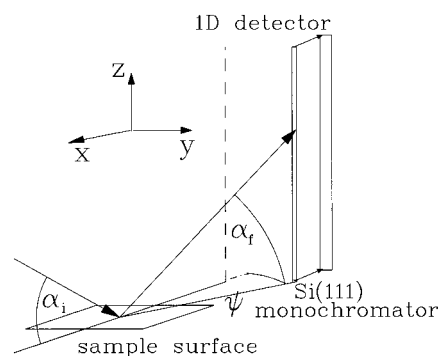


**Figure 1.** Schematic view of the experimental setup used for the off-specular X-ray scattering measurements. The incident angle is denoted $\alpha_i$, the exit angle $\alpha_f$, and the out-of-plane angle $\psi$. A Si(111) analyzer crystal increases the resolution in the out-of-plane direction. A one-dimensional detector is used to measure one complete detector or off-detector scan.

a flat reference surface and the investigated sample is recorded in an area detector while the reference plane is moved with a piezoelectric device. This enables a lateral resolution of approximately 1 $\mu$m and a height resolution better than 10 Å. A magnification of 10 and 100 times was used. The area from which a data analysis is performed was 600 $\mu$m × 800 $\mu$m and 42.2 $\mu$m × 42.2 $\mu$m, respectively.

**X-ray Reflectometry:** The specularly scattered intensity was measured using a laboratory X-ray source ($\lambda$ = 1.54 Å, $\theta$−$\theta$ reflectometer Seifert XRD 3003TT). The combination of a Ge(110) channel cut monochromator crystal in front of the sample and a slit collimation in front of the detector enables the detection of reflected intensities up to 8 orders of magnitude. The sample is placed on a horizontally mounted vacuum chuck. It is measured at room temperature under air. Reflectivity measurements were used to characterize all samples right after preparation. From a fit to the data,[18−20] the total film thickness and the surface and interface roughness are determined. In the model used for this fit each interfaces between homogeneous layers is described by a tanh refractive index profile. The width of the profile yields the interfacial roughness $\sigma$. Commonly in the literature the interface of polymers[21] and silicon substrates[22] is described by a tanh profile. In the case of polymer interfaces it is based on the volume fraction profile $\Psi$ which can be described by a tanh profile to a good approximation.[23] Deviations originating from a concentration dependence of $\chi$ or the limited validity of the used approximations in the calculation of $\sigma$[24] are neglected.

**X-ray Off-Specular Scattering.** The diffusely scattered intensity was recorded at the Troika II beamline (ID10B) at the ESRF in Grenoble. The setup for scattering in-plane and out-of-plane reflections is shown in Figure 1. The sample was placed onto a two-axis goniometer with a *x*, *y*, *z*-translation stage in a special designed sample cell. We used a wavelength of 1.548 Å of the undulator and a two-slit collimation system in front of the sample. A one-dimensional linear detector was placed in a distance of 671 mm behind the sample. Because of the Si(111) analyzer crystal a resolution of 3.54 × $10^{-4}$ Å$^{-1}$ was achieved. At one fixed angle of incidence $\alpha_i$ in the plane of reflection either a detector scan ($\Psi$ = 0) or out-of the plane of reflection an off-detector scan ($\Psi \neq 0$) was measured. The combination of crystal optics and a one-dimensional detector allows us to measure the off-specularly scattered intensity at large *q* values as compared to other setups.

## Roughness Replication

A single interface *j* is described by a contour function $h_j(\bar{p})$ with the lateral vector $\bar{p}$. A statistical description is yielded from the height−height correlation function[25]

$$C_j(\bar{r}) = \langle h_j(\bar{r} + \bar{p})\, h_j(\bar{p}) \rangle = \lim_{A \to \infty} \int\int_A \mathrm{d}\bar{p}\, h_j(\bar{r} + \bar{p}) h_j(\bar{p}) \rangle \bar{p}$$

(1)

In the case of several interfaces a correlation between them becomes possible. If at least the interface contour is partially transferred from one layer to the next, in addition a cross-correlation function $C_{jk}$ has to be taken into account.[26] In Fourier space a replication function $\chi_{jk}(\bar{q})$ is defined, which describes the transferred part of the roughness spectrum[27]

$$\tilde{h}_k(\bar{q}) = \chi_{jk}(\bar{q})\, \tilde{h}_j(\bar{q}) + \tilde{w}_k(\bar{q}) \qquad (2)$$

The intrinsic part of the roughness spectrum is denoted with $\tilde{w}_k(\bar{q})$. A fully or partial correlation between different interfaces $j$ and $k$ gives rise to constructive interference between diffusely scattered beams from different interfaces.[28] Thus, intensity is enhanced in sheets parallel to the $q_z$ axis.[29] This so-called resonant diffuse scattering is in phase with the Kiessig fringes of the reflectivity curve.[30] As a consequence the distance between maxima of the diffusely scattered intensity is given by $2\pi/(z_j - z_k)$ and reflects the distance $l^{corr} = z_j - z_k$ of the correlated interfaces. If in a scan through the reciprocal space these sheets of enhanced intensity are cut, they are visible as modulations. Advantageous is the detector scan: The sample is held fixed at one angle of incidence $\alpha_i$ and the detector position is varied around the specular peak. Depending on the angular range measured in addition to possible modulations due to resonant diffuse scattering, the specular peak and the Yoneda peak are visible. The Yoneda peak is a typical dynamic feature of diffuse scattering,[31] which arises from an enhancement of the scattered intensity, if the incident or exit angle equals the critical angle $\alpha_{i,f} = \alpha_c$ due to a standing wave field. This standing wave field can cause interference fringes created by a waveguide behavior of two interfaces separated by a distance $l^{dyn}$. The Yoneda peak can be regarded as the zeroth order. The different angular dependences of both mechanisms enable the separation within a detector scan.[30] As a consequence one single detector scan is sufficient to detect roughness replication.

If only a part of the roughness spectrum is transferred, it is convenient to introduce a lower cutoff length $\xi$. In reciprocal space, the sheets of enhanced intensity extend laterally up to a maximum wavevector $q_{max} = 2\pi/\xi$. From the decay of the fringes in off-detector scans this value of $q_{max}$ is determined. In contrast to the detector scans, off-detector scans are measured out of the plane of reflection at $\Psi \neq 0$. Other characteristic features of the detector scan, namely the Yoneda and the specular peak, are present in the off-detector scans as well. Whereas the specular peak is basically given by the resolution function, the Yoneda peak contains a convolution of the resolution function with a function depending on the power spectral density function of the effective surface.

In the case of a nonisotropic surface the off-specular scattering depends strongly on the sample position. Thus, the measured intensity distribution will change if the sample is shifted in the beam. Therefore, measurements at different sample positions or orientations are a common test.

## Results and Discussion

**Polymer Film Surface.** The information perpendicular to the sample surface is obtained from the fit of the reflectivity data. Basically the depth dependence of the density profile is probed over the coherently il-
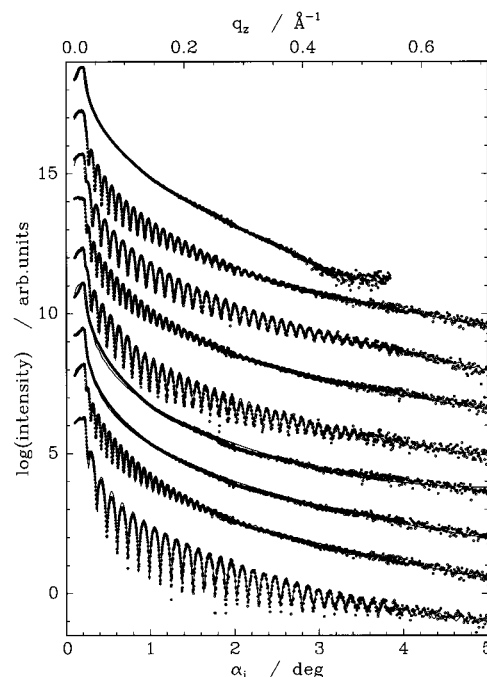


**Figure 2.** Specular X-ray reflectivity curves (dots) together with a fit to the data (solid lines) picturing the influence of the used solvent. During the preparation of all thin films the amount of PS used was kept constant. From the bottom to the top the solvent was changed as denoted in the text. The curves are shifted by 1.5 orders of magnitude against each other to clarify the observed shape.

luminated sample surface.[32] Averaged information like the surface roughness, the mean density and the film thickness are obtained.

In sample series A the type of solvent used for the spin coating was varied, and the amount of polymer PS used was kept constant. Figure 2 shows the reflectivity data (dots) and the corresponding fit (solid line) using the model described above. From the bottom to the top the solvents used are toluene, tetrahydrofuran, cyclohexane at 50 °C, a mixture of acetone and cyclohexane, 1,2-dichloroethane, chloroform, trichloroethylene, a mixture of cyclohexane and toluene, and a mixture of methanol and toluene. Already from the reflectivity curves, it is obvious that quite different films were formed. The observed data differ in the width and the depth of the fringes which corresponds to different film thicknesses and surface roughnesses. Several reflectivity curves exhibit no fringes at all. In the topmost curve, the measured reflectivity is equal to the one of the bare substrate. Thus, from the preparation out of a mixture of methanol and toluene no PS film results. Although the third and fourth reflectivity scans from the bottom show no fringes as well, the intensity decay as a function of incident angle $\alpha_i$ is different from the one of the bare substrate. Consequently a very rough PS film is present, if cyclohexane or a mixture of cyclohexane and acetone is used. From the fit to the reflectivity data the film thickness $l$ and surface roughness $\sigma$ is only roughly determined to be $l \cong 500$ Å and $\sigma \cong 45$ Å. The value of the surface roughness agrees well with the one obtained from optical phase interference microscopy. It results from a well-pronounced surface pattern. Figure 3 shows the evolved surface morphology of thin films prepared from a cyclohexane solution (Figure 3a) and from a mixture of cyclohexane and acetone (Figure 3b). Both micrographs exhibit a part of the sample which is not
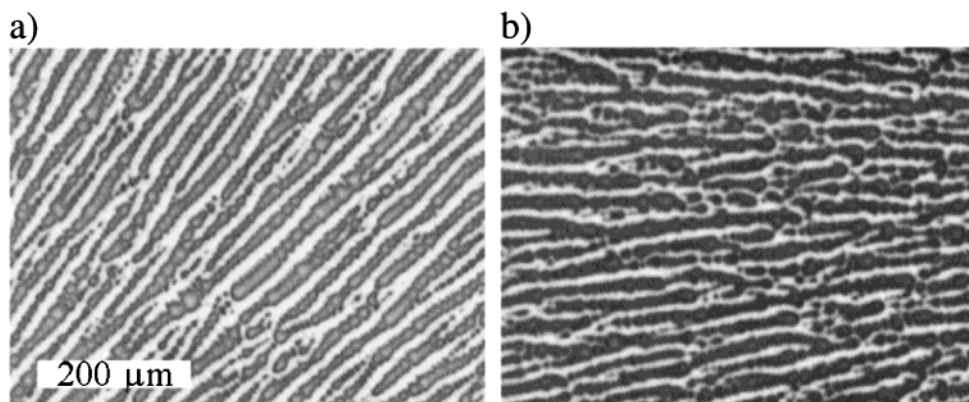
**Figure 3.** Optical micrographs of surface morphologies introduced by using cyclohexane (a) and a mixture of cyclohexane and acetone (b). The used polymer is PS. Both micrographs are recorded with a magnification of 10 times. The whole picture covers a range of $625 \times 469 \ \mu m^2$.

directly in the center of the rotation and thus a marked striped topography is observed. It results from hydrodynamic instabilities which occur in the spin-coating process during the stage which is dominated by a hydrodynamic flow field. Using different solvents smooth and homogeneous PS films with film thicknesses between 340 (toluene) and 630 Å (THF) were obtained. As already visualized by the depth of the fringes (bottom curve in Figure 2), spin coating using a toluene solution yields the smallest surface roughness of $\sigma = 3$ Å. Values of 4 Å have been achieved using 1,2-dichlorethane and trichloroethylene. For the mixture of cyclohexane and toluene the roughness increases to 8 Å and for THF to 9 Å, respectively. Neither with optical microscopy nor with optical phase interference microscopy are surface morphologies observable. The example of the mixture of cyclohexane and toluene shows that by adding a small amount of a different solvent, the resulting surface morphologies are completely changed. If smooth films are desirable, the roughness is reduced by a factor of 7 by adding toluene. Thus, the creation of surface morphologies is overcome in this mixture as compared to cyclohexane as a pure solvent.

In sample series B, PBrS is used instead of PS. The polymer concentration was varied to obtain thin films with constant film thickness. The resulting reflectivity data look very similar to the ones presented in Figure 2, however, with a few exceptions. Because cyclohexane does not dissolve PBrS, we do not obtain even a rough polymer film. The measured film thickness of the remaining samples is $l = 340 \pm 17$ Å. The given error bar includes the deviations from samples prepared out of different solutions. To reduce this value of $\pm 17$ Å significantly, an increased number of samples would have been necessary, because the relation between the amount of polymer used and the resulting film thickness is still only known with the uncertainty of a prefactor.[6] On the other hand typical parameters like surface roughness or film morphology are not significantly affected by these small deviations. The measured values of the surface roughness are similar to the ones from the PS series.

To find out a possible origin of the observed values, we analyze the surface roughness $\sigma_{rms}$ as a function of the characteristic parameters of the solvents used, as listed in Table 1. In Figure 4a $\sigma_{rms}$ is plotted as a function of the vapor pressure $v_p$ of the solvent. With increasing vapor pressure, the surface roughness
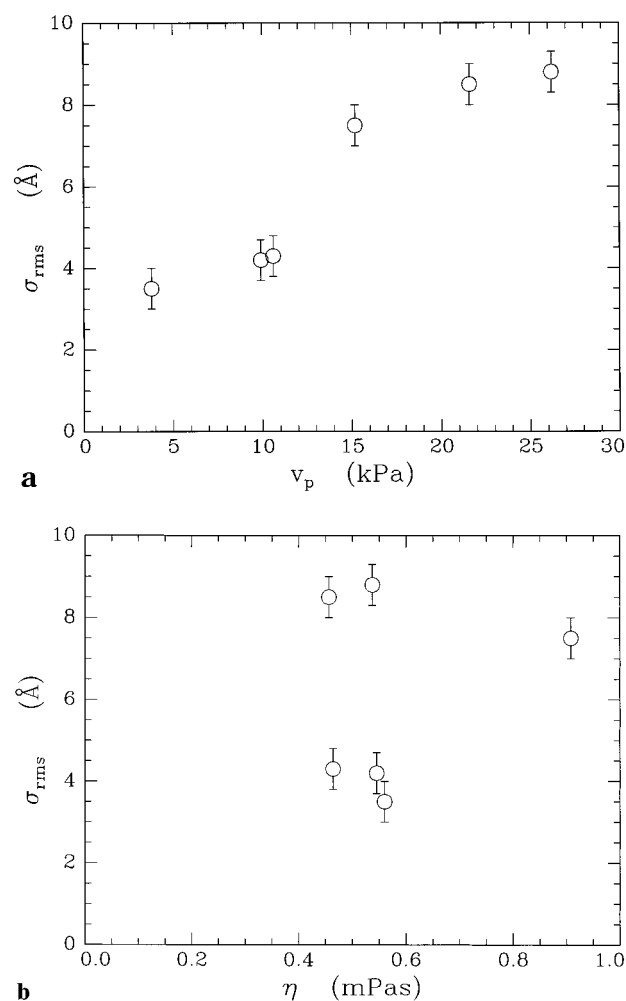


**Figure 4.** (a) Surface roughness $\sigma_{rms}$ plotted as a function of the vapor pressure $v_p$ of the solvent used. (b) Surface roughness $\sigma_{rms}$ plotted as a function of the viscosity $\eta$. The solvents used can be identified with the help of Table 1.

increases as well. We detect no simple functional dependence, though, which stresses the complexity of the spin-coating process. A similar result was obtained in earlier works only quite qualitatively.[5] Compared to the vapor pressure the viscosity $\eta$ of the solvent does not play a significant role. In Figure 4b, $\sigma_{rms}$ is shown as a function of $\eta$. Not even a clear trend of possible dependence is observable, although the viscosity is believed to be important as well.[5] Similarly no depen-

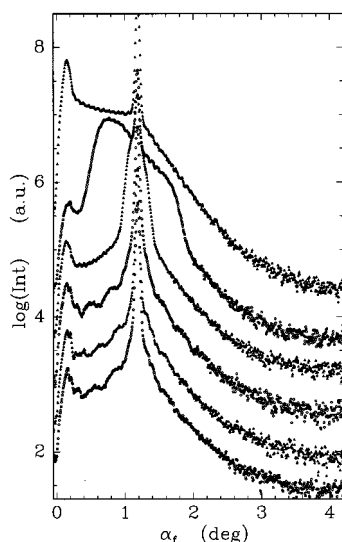**Figure 5.** Detector scans measured at an incident angle $\alpha_i = 1.2°$ picturing the different morphologies observed in this investigation. From the bottom to the top the solvent was changed as denoted in the text. The used polymer is PBrS. All curves are shifted for clarity against each other by a constant order of magnitude.

dence from the other parameters listed in Table 1, namely the surface tension or the electric dipole moment can be extracted.

Of course, a direct relation between the observed film parameters and the characteristic solvent parameters has to be understood as a simplification. The solvent parameters are modified by the dissolving of the polymers[33] and continuously changed during the spin-coating procedure due to solvent evaporation. For example, already in the solution used at the start of the spin coating, the viscosity is enhanced due to even small amounts of dissolved polymer. In addition with increasing molecular weight of the polymer the viscosity increases as well, e.g. from $1.12 \times 10^{-3}$ Pa s for PS23K in toluene to $5.55 \times 10^{-3}$ Pa s for PS186K in toluene.[5] On the other hand the amount of the polymer used was

kept constant or only varied in a small range, which results in only very small changes. During the spin coating the viscosity change basically addresses the kinetics of the film creation which is not determined here. Since we investigated only the final static structures, plots like Figure 4, parts a and b, seem still meaningful.

**Long-Range Correlation.** Utilizing off-specular scattering, long-range correlations are determined, which are no longer visible with optical methods. Figure 5 shows examples of detector scans measured for thin PBrS films (sample series B). In general PS films show a similar behavior. From the bottom to the top the used solvents are toluene, trichloroethylene, 1,2-dichloroethane, chloroform, tetrahydrofuran, and carbon tetrachloride. The presented data depict nicely the observed types of long-range correlation. The top curve in Figure 5 exhibits only the specular peak at $\alpha_f = 1.2°$ and the Yoneda peak at $\alpha_f = 0.2°$, without further features of the diffuse scattering. Thus, no long-range correlation is present. In curves two and three from the top, the diffuse scattering is symmetrically increased around the specular peak, which is a sign of an in-plane correlation with a single most prominent length on the order of micrometers. In the bottom three curves, modulations of the diffusely scattered intensity are visible in addition to the specular and to the Yoneda peak. As described in the section about roughness replication, these modulations originate from resonant diffuse scattering and thus are a fingerprint of strongly correlated interfaces. The differences in the spacing of the fringes result from the slight differences of the film thickness.

After being annealed above the glass transition temperature, the polymer surface is statistically independent from the substrate,[7] despite a small part of the substrate roughness which is transferred through the film.[34] Consequently no long-range correlation is dominant. Right after preparation by spin coating, it was shown recently that independent surface morphologies are obtainable by basically three different mechanisms.[9] PBrS films prepared from a tetrahydrofuran solution
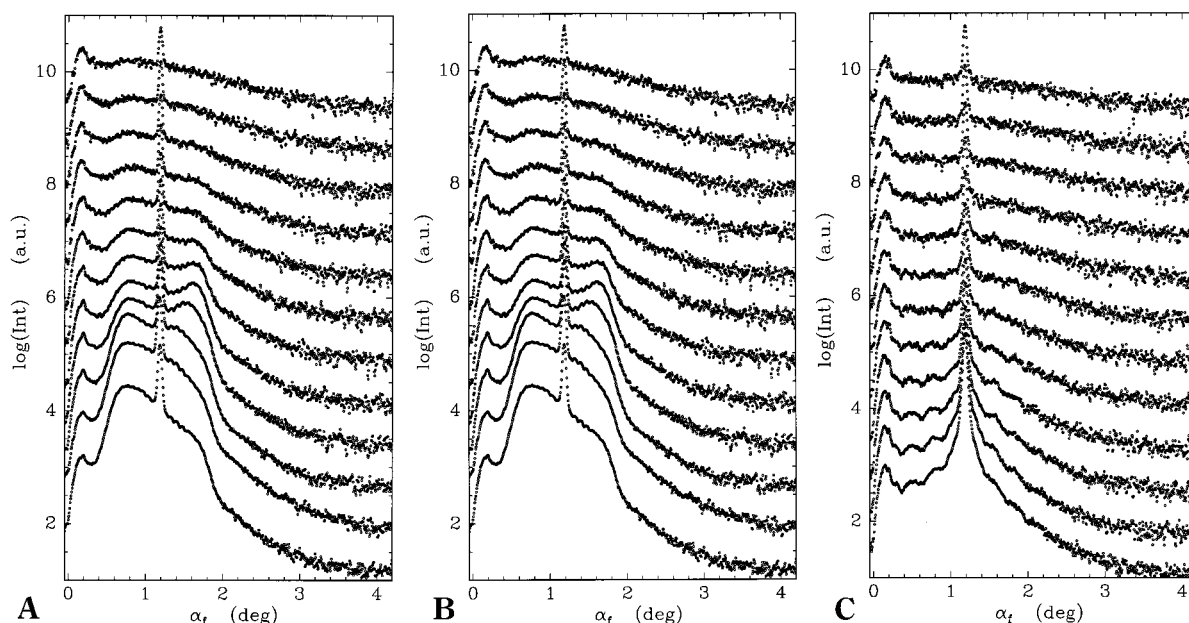


**Figure 6.** Off-detector scans showing the evolution of the modulation resulting from resonant diffuse scattering as a function of increasing $q_y$ (from the bottom to the top): (a) carbon tetrachloride, (b) chloroform, and (c) 1,2-dichloromethane. The polymer used is PBrS.
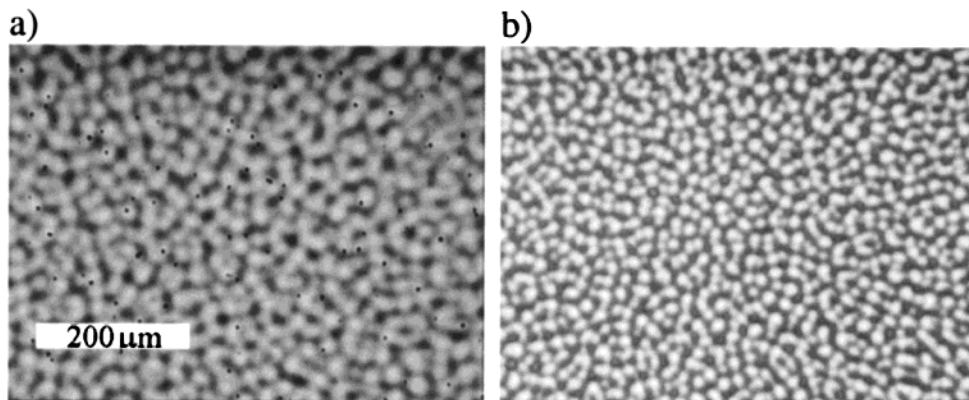
**Figure 7.** Optical micrographs of surface morphologies introduced by using chloroform (a) and carbon tetrachloride (b) as common solvents. The used polymer is PBrS. Both micrographs are recorded with a magnification of 10 times. The whole picture covers a range of $625 \times 469 \, \mu m^2$.

have no well pronounced surface roughness which is quantified by the small value $\sigma = 9$ Å, but the film thickness is inhomogeneous over areas of several micrometers. PS films exhibit the same behavior. During the preparation no hydrodynamic instabilities are introduced, which would generate a starlike pattern centered at the center of rotation. The vapor pressure is sufficiently high to freeze in an uniform film without roughness replication. Thus, the polymer surface is not determined by the substrate. As a consequence only the specular and the Yoneda peaks are observed in a detector scan.

The presence of well-defined in-plane morphologies gives rise to additional intensity contributions at a position characteristic for the related in-plane length. While in a rocking scan (sample moved at fixed detector position) this is observable as a symmetrical increase of the intensity with respect to the specular peak, in a detector scan this symmetry is no longer valid, due to the parabolic path through reciprocal space. Only the small $q_x$ component in a detector scan is responsible for possibility of detecting large in-plane lengths. Using carbon tetrachloride as well as chloroform results in this type of scattering. The dominant in-plane lengths are $\xi_{\parallel} = 0.72 \, \mu m$ for $CCl_4$ and $\xi_{\parallel} = 3.15 \, \mu m$ for $CHCl_3$. In Figure 6, parts a and b, the $q_y$ dependence is displayed in several off-detector scans. Because of the high vapor pressure of $CHCl_3$, a highly viscous polymer−solvent layer on top of more dilute solution is established during the preparation. In highly viscous solutions, the fluid flow is no longer Newtonian, and thus even an initially uniform film is deformed by the rotation.[35] Hydrodynamic instabilities which create surface morphologies are frozen in at earlier stages of the spin-coating process. Only at a smaller vapor pressure is the diffusion sufficiently high to enable homogeneous surfaces. Because the solution still behaves like a Newtonian liquid, possible irregularities of the surface contour are smoothed out by the centrifugation.[35] In Figure 7 the morphologies as observed with optical microscopy are shown. Despite a different lateral dimension, both are of similar types.

For a given wavevector interval of the surface roughness spectrum of the substrate, a vertical correlation between the substrate surface and the polymer surface is installed due to the preparation procedure. While for thin films prepared out of a toluene solution this was reported previously,[7,8] the two other examples show that even with other solvents like trichloroethylene and 1,2-
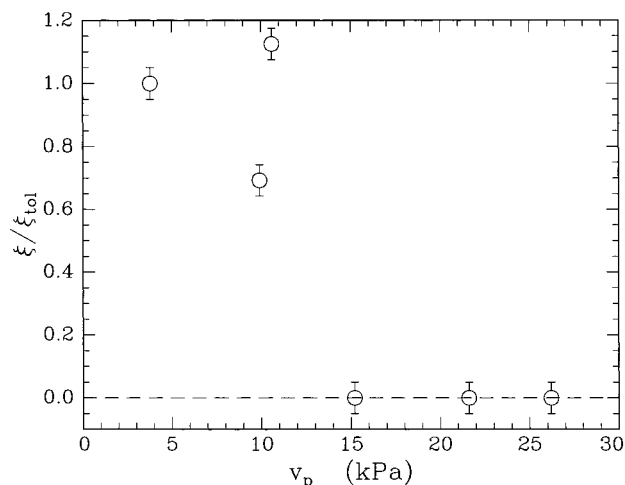


**Figure 8.** Cutoff length $\xi$ normalized by the value determined for toluene $\xi_{tol}$ as a function of the vapor pressure of the solvent. The used polymer is PBrS. The solvents used can be identified from Table 1.

dichloroethane, it is possible to produce this morphology. Thus, the special case of a locally constant film thickness is not only limited to the use of toluene only. Figure 6c shows the $q_y$ dependence of the observed modulations for the example of 1,2-dichloroethane. From the bottom to the top $q_y$ increases, and thus, smaller in-plane distances are probed with respect to the long-range correlation. From the vanishing of the modulation in the off-detector scans the lower cutoff length $\xi$ is determined. In Figure 8 this length as determined from the data, normalized by the value of toluene, is plotted as a function of the vapor pressure. For samples which exhibit no interface correlation $\xi$ was set to zero. We chose the well-investigated solvent toluene as a reference. Figure 8 suggests that for the used preparation parameters there seems to exist a maximum value of the vapor pressure up to which the creation of homogeneous, correlated films is possible.

## Summary

The solvent used during the preparation of thin polymer films via spin-coating has a big influence on the resulting morphologies. Solvents with low vapor pressure as well as solvents with high vapor pressure are useful for the preparation of smooth polymer surfaces. In an intermediate vapor pressure range, marked surface structures are created. These morphol-

ogies give rise to a large surface roughness and nonhomogeneous polymer films. Films prepared out of very volatile solvents like THF are not that smooth as compared to the ones prepared out of weakly volatile solvents. In the case of toluene, trichloroethylene, and 1,2-dichloroethane the smoothness of the polymer film is limited by the roughness of the underlying substrate. Because of the roughness replication a large part of the roughness spectrum of the substrate, down to typical in-plane lengths on the order of 1000 Å, dominates the morphology of the polymer film. This suggests that one way to produce even smoother polymer films is given by the use of more perfect substrates. For silicon substrates roughness values down below 1 Å have been published. We showed that beside the reported solvent toluene, also other solvents give rise to films with correlated roughness. This metastable, energetically unfavorable state is due to the nonequilibrium nature of the spin-coating process. Consequently the formation of long-range correlations perpendicular to the substrate surface is not restricted to one special solvent with one special set of physical parameters. This suggests that roughness correlation is not only limited to model systems. Hence, a locally constant film thickness may also be formed with other solvents and polymers. Using solvent mixtures the disadvantageous properties of one single solvent like cyclohexane can be overcome. By simply adding an amount of toluene, the creation of marked surface morphologies is suppressed. We note that roughness correlation was not observed by using solvent mixtures so far.

## References and Notes

(1) Bornside, D. E.; Macosko, C. W.; Scriven, L. E. *J. Imag. Technol.* **1987**, *13*, 122.
(2) Lawrence, C. J. *Phys. Fluids* **1988**, *31*, 2786.
(3) Oron, A.; Davis, S. H.; Bankoff, S. G. *Rev. Mod. Phys.* **1997**, *69*, 931.
(4) Meyerhofer, D. *J. Appl. Phys.* **1978**, *49*, 3993.
(5) Spangler, L. L.; Torkelson, J. M.; Poyal, J. S. *Polym. Eng. Sci.* **1990**, *30*, 644.
(6) Schubert, D. W. *Polym. Bull.* **1997**, *38*, 177.
(7) Müller-Buschbaum, P.; Stamm, M. *Macromolecules* **1998**, *31*, 3686.
(8) Müller-Buschbaum, P.; Gutmann, J. S.; Lorenz, C.; Schmitt,T.; Stamm, M. *Macromolecules* **1998**, *31*, 9265.
(9) Müller-Buschbaum, P.; Gutmann, J. S.; Kraus, J.; Walter, H.;Stamm, M. *Macromolecules* **2000**, *33*, 569.
(10) Salditt, T.; Rhan, H.; Metzger, T. H.; Peisl, J.; Schuster,R.; Kotthaus, J. P. *Z. Phys. B* **1995**, *96*, 227.
(11) Salditt, T.; Metzger, T. H.; Peisl, J.; Goerigk, G. *J. Phys. D: Appl. Phys.* **1995**, *28*, A236.
(12) Salditt, T.; Metzger, T. H.; Brandt, Ch.; Klemradt, U.; Peisl, J. *Phys. Rev. B* **1995**, *51*, 5617.
(13) Müller-Buschbaum, Casagrande, M.; Gutmann, J. S.; Kuhlmann,T.; Stamm, M.; Cunis, S.; von Krosigk, G.; Lode, U.; Gehrke, R. *Europhys. Lett.* **1998**, *42*, 517.
(14) Brandrup, J.; Immergut, E. H. In *Polymer Handbook*, 3rd ed.; John Wiley & Sons: New York, 1989.
(15) *CRC Handbook of Chemistry and Physics*, 78th ed.; Linde, D. R., Frederikse, H. P. R., Eds.; CRC Press Inc.: New York, 1997.
(16) Kambour, R. P.; Bendler, J. T.; Bopp, R. C. *Macromolecules* **1983**, *16*, 753.
(17) Kambour, R. P.; Bendler, J. T. *Macromolecules* **1986**, *19*, 2679.
(18) L. G. Parrat, *Phys. Rev.*, **1954**, *55*, 359.
(19) Born, M.; Wolf, E. In *Principles of Optics*, 2nd ed.; Pergamon Press: Oxford, England, 1964.
(20) James, R. W. In *The Optical Principles of the Diffraction of X-rays*; OxBow Press: Woodbridge, CT, 1962.
(21) Stamm, M.; Schubert, D. W. *Annu. Rev. Mater. Sci.* **1995**, *25*, 325.
(22) Bahr, D.; Press, W.; Jebasinski, R.; Mantl, S. *Phys. Rev. B*, **1993**, *47*, 4385.
(23) Binder, K. *J. Chem. Phys.* **1983**, *79*, 6387.
(24) Binder, K.; Frisch, H. *Macromolecules* **1984**, 17, 2928.
(25) Yaglom, A. M. *Correlation theory of stationary and related random functions*; Springer Series in Statistics; Springer Verlag: New York, 1987.
(26) Stettner, J.; Schwalowsky, L.; Seeck, O. H.; Tolan, M.; Press, W.; Schwarz, C.; Känel, H. v. *Phys. Rev. B* **1996**, *53*, 1398.
(27) Spiller, E.; Stearns, D.; Krumrey, M. *J. Appl. Phys.* **1993**, *74*, 107.
(28) Sinha, S. K.; Sirota, E. B.; Garoff, S.; Stanley, H. B. *Phys. Rev. B* **1988**, *38*, 2297.
(29) Daillant, J.; Bélorgey, O. *J. Chem. Phys.* **1992**, *97*, 5824.
(30) Holý, V.; Baumbach, T. *Phys. Rev. B* **1994**, *49*, 10668.
(31) Yoneda, Y. *Phys. Rev.* **1963**, *131*, 2010.
(32) Parrat, L. G. *Phys. Rev.* **1954**, *55*, 359.
(33) Irzhak, V. I. *Int. J. Polym. Mater.* **1980**, *8*, 201.
(34) Andelman, D.; Joanny, J. F.; Robbins, M. O. *Europhys. Lett.* **1988**, *7*, 731.
(35) Acrivos, A.; Shah, M. J.; Petersen, E. E. *J. Appl. Phys.* **1960**, *31*, 963.

MA0009193